C-CORE PUBLICATION No. 90-24.

INTERNATIONAL ASSOCIATION FOR
GREAT LAKES RESEARCH

J. Great Lakes Res. 17(1):120-131
Internat. Assoc. Great Lakes Res., 1991

AN ACOUSTIC PARAMETRIC ARRAY FOR MEASURING THE THICKNESS AND STRATIGRAPHY OF CONTAMINATED SEDIMENTS

J. Y. Guigné[1], N. Rukavina[2], P. H. Hunt[1], and J. S. Ford[2]

[1]Centre for Cold Ocean Resources Engineering
Memorial University of Newfoundland
St. John's, Newfoundland A1B 3X5

[2] Environment Canada
Canada Centre for Inland Waters
National Water Research Institute
867 Lakeshore Road
Burlington, Ontario L7R 4A6

J. Great Lakes Res. 17(1):120–131
Internat. Assoc. Great Lakes Res., 1991

AN ACOUSTIC PARAMETRIC ARRAY FOR MEASURING THE THICKNESS AND STRATIGRAPHY OF CONTAMINATED SEDIMENTS

J. Y. Guigné[1], N. Rukavina[2], P. H. Hunt[1], and J. S. Ford[2]

[1]Centre for Cold Ocean Resources Engineering
Memorial University of Newfoundland
St. John's, Newfoundland A1B 3X5

[2] Environment Canada
Canada Centre for Inland Waters
National Water Research Institute
867 Lakeshore Road
Burlington, Ontario L7R 4A6

ABSTRACT. *Acoustic mapping and monitoring of thin contaminated sediments in inland waters requires an optimized acoustic source. An experiment conducted in Hamilton Harbour, Lake Ontario, demonstrated that high resolution recording of sediment layering is possible when a parametric acoustic source is used. Good correlation was obtained with the stratigraphy of cores from the test site, and parametric records revealed a 4 cm ooze layer at the surface that could not be resolved using a conventional acoustic source. The encouraging performance of the parametric source for measuring thickness of sediments, which are typically not amenable to acoustic measurement, suggests that an acoustic parametric array might be a useful tool for monitoring sedimentation processes or for high-resolution surveys of modern sediment thickness and volume.*
INDEX WORDS: Stratigraphy, acoustics, lake sediments, sediment distribution.

INTRODUCTION

Contaminated-sediments research in inland waters depends upon reliable data on the thickness and geometry of the polluted sediments and the physical processes which lead to their transport and accumulation. Data are needed to guide field sampling, to map the volume and distribution of contaminants and their changes through time, and, ultimately, to develop the strategy for cleanup.

Acoustic techniques provide a rapid, non-destructive method of examining contaminated sediments. If changes in the acoustic response of the sediments can be correlated with changes in their physical properties, then acoustics can provide insight into sediment transport processes and into the mechanisms of entrapment of pollutants.

Past attempts at mapping these sediments acoustically with conventional hydrographic sounders have not been successful in detecting the thin, water-rich surficial layers (Guigné *et al.* 1990). This paper describes an improved sounder based on a parametric array source. Tests of the array were conducted in Hamilton Harbour, Lake Ontario, to compare its performance with that of a conventional sounder. Cores collected at a test site showed that the parametric source was able to detect thin surface layers that could not be resolved by the conventional sounder and suggest that it may have some potential in environmental research as a tool for mapping and monitoring of modern polluted sediments.

CRITERIA FOR ACOUSTIC SOUNDING

Common acoustic sources provide a burst of acoustic energy which propagates normal to the lakebed. The sudden change in acoustic properties between the water and lakebed causes a proportion of the incident energy to be reflected. The proportion of energy reflected depends upon the roughness of the reflecting surface and the normal incidence reflection coefficient. In cases where a lakebed appears smooth in terms of the acoustic wavelengths, the reflection coefficient is merely the acoustic impedance contrast between the two

92-01851/

media. A number of studies on the relationships between physical properties of sediments such as porosity, median grain size, and reflectivity are available (Smithy and Li 1966, Fass 1969, Hamilton 1974, Orr and Rhoads 1982). In general, reflectivity bears an inverse relationship to porosity. High porosity is associated with fine grained sediments and low porosity with coarse grained sediments; clays tend to be poor reflectors while sands tend to be good reflectors (Pace and Ceen 1982). Acoustic energy that is not reflected at the water/lakebed interface is transmitted through the sedimentary column until it reaches another acoustic impedance contrast and then a proportion of that energy is again reflected.

The characteristics of an acoustic source dictate the temporal and hence vertical resolution of an acoustic sounding system. The length of an acoustic pulse, which is determined by a signal's bandwidth, places limits upon the minimum thickness of a layer that a system can resolve distinctly. When an acoustic pulse length is of the same order as the layer thickness, the returns from the top and bottom of the layer interfere making it impossible to discern the two events coherently. The source characteristics also dictate the receiving and recording devices used. The short pulse, which is required to achieve a high resolution, produces a high frequency content and bandwidth in the source wavelet. This high frequency content places limits on the type of hydrophone and digital recorder which can be used. Most hydrophones have a response which is linear at low frequencies but becomes nonlinear in the high kilohertz range. In cases where the source wavelet's frequency content resides in this nonlinear portion of the hydrophone's response spectrum, the exact response function must be known such that its effect can be removed from the recorded data. Signal theory demands at least two samples per cycle for the preservation of frequency information in digital recording. When this is violated the aliased frequencies become folded back into the spectrum, contaminating the data. This means that the digitizer must have a sampling frequency of at least twice that of the highest frequency in the source wavelet.

The amplitude of the source wavelet decays as a function of time and material. This decay is due to spherical divergence and inelastic attenuation. Spherical divergence is the result of the geometric spreading that results as a wave travels. This can be visualized if one considers the source as a point source. When the source generates an acoustic pulse, the energy travels radially away forming a spherical wavefront around the origin. The energy in the wave is spread over a larger area with time. Since energy density is inversely proportional to the square of the radius of the sphere, and amplitude is proportional to the square root of the energy, spherical divergence is inversely proportional to the radius of the sphere.

Inelastic attenuation occurs as energy in the wave is transformed into heat energy. The mechanisms by which the elastic energy is transformed into heat are not understood clearly. During the passage of a wave, heat is generated in the compressive phase and absorbed in the expansive phase. The process is not perfectly reversible since heat lost during compression is greater than that which is gained during expansion. Internal friction and viscous dissipation in pore fluids undoubtedly play a major role in the process (Telford *et al.* 1976).

Although absorption is a complex subject, empirical relationships have been established between the absorption coefficient and the physical properties of sediments in marine environments (Hamilton 1971, 1972; Hamilton and Bachman 1982). While the mechanisms are still not clearly understood it is generally agreed that absorption increases with frequency. If we consider the processes involved it can be seen that reflected energy will represent only a small portion of the source delivery. The loss of amplitude due to both types of attenuation will make the dynamic range of the data acquisition digitizer a factor to consider. The amplitude resolution in the recorded data set is dependant on the available dynamic range. The larger the dynamic range the more faithfully small variations in amplitude in the analogue signal can be represented in digital format. Clearly a tradeoff occurs between temporal resolution and depth of penetration, with the former requiring broad band, high frequencies and the latter requiring low frequencies.

PARAMETRIC ARRAY

It is desirable that the temporal resolution of a sound source be such as to prevent interference between thin layers. A short and narrow beam signal will also provide better signal-to-reverberation ratios when scattering is present in the medium. However, such pulses are rarely achievable using conventional seismic profilers. The development

of the parametric array allows for such a broadband source to be realized in practice (Berktay *et al.* 1979).

The fundamental principles of the parametric array were first described by Westervelt (1963), where the nonlinear interaction of sound in water was presented. If two intense sound beams were coaxially transmitted into the water, the nonlinearity of the water medium generated new secondary frequencies which were sums and differences of the primary propagation frequencies. A very narrow beam was produced at the low difference frequencies. The bandwidth for these frequencies was found to be large, approximately that of the primaries. An efficient technique for generating such a broadband parametric array is to employ a process called self demodulation (Berktay 1965). If a modulated carrier frequency signal is radiated from the acoustic transducer, nonlinear interaction takes place in the water between all frequency components present, by virtue of the modulation envelope. The secondary signal thus produced in the water contains a band of difference frequencies and has a time domain form proportional to the second time derivatives of the square of the modulation envelope. The secondary pressure produced by a parametric array may be expressed as:

$$p(\vec{r}, t) = D \frac{\partial^2}{\partial t^2} p^2_m(t) * i(\vec{r}, t) \qquad (1)$$

where i(r, t) is the impulse response of the parametric array at position r and D is a constant (Ceen and Pace 1981, Pace and Ceen 1983). For subbottom profiling, the axial waveform of the parametric array is normally incident on the water/sediment interface in the nearfield of the carrier frequency. The impulse response of the axis may often be taken as a delta function and will be assumed to be so here. The primary frequency modulation is $p_m(t)$ and may take many forms, depending on the application. For a broadband secondary signal, a form for $p_m(t)$ which is easily implemented is the cosine bell:

$$pm(t) = \frac{1}{2} (1 + \cos 2\pi f_c t) \left[U(t + \frac{1}{2f_c}) - U(t - \frac{1}{2f_c}) \right] \quad (2)$$

where U(.) is the unit step function and f_c is the carrier frequency. The normalized on-axis secondary waveform resulting from this modulation is

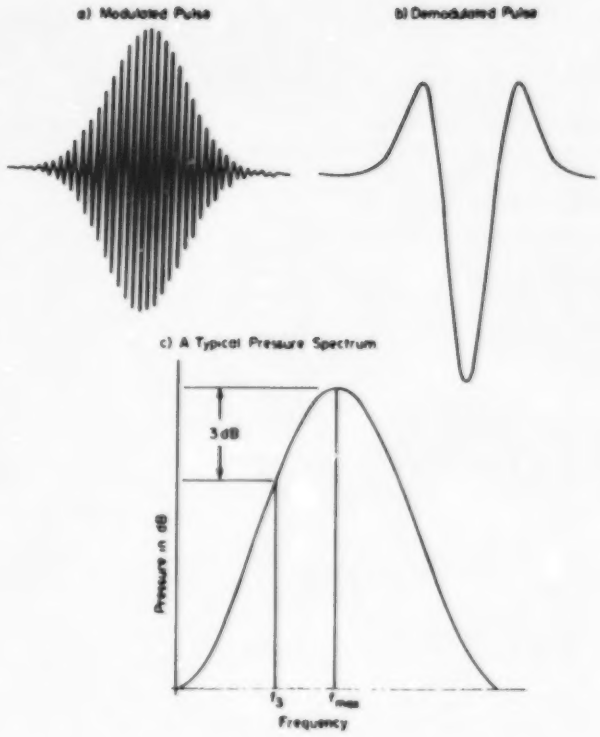

FIG. 1. Modulated signal with its resultant inverse Ricker wavelet generated through self-demodulation (a and b). Typical pressure spectrum of a demodulated signal (c—after Guigné et al. *1989).*

$$p(t) = \frac{1}{2} (\cos 2\pi f_c t + \cos 4\pi f_c t) \left[U(t + \frac{1}{2f_c}) - U(t - \frac{1}{2f_c}) \right] \quad (3)$$

This waveform has a normalized spectrum

$$P_o(f) = \frac{\pi f}{2f_c} \left[\frac{\sin A}{A} \frac{1}{(2 + f/f_c)} + \frac{\sin B}{B} \frac{1}{(1 + f/f_c)} \right] \quad (4)$$

where $A = (2 - f/f_c)$ and $B = (1 - f/f_c)$. This spectrum peaks at $f = 1.5\ f_c$. Figure 1 shows a "raised cosine bell" modulated carrier and the self-demodulation signal which would be received on a broadband hydrophone located on the acoustic axis of the transmitting transducer. The pressure spectrum of the secondary of demodulated signal is also shown in this figure (Guigné *et al.* 1989).

Sensor Configuration and Location

The acoustic system used in this study was developed at C-CORE, Memorial University (Guigné 1986, Guigné and Chin 1989). The device consisted

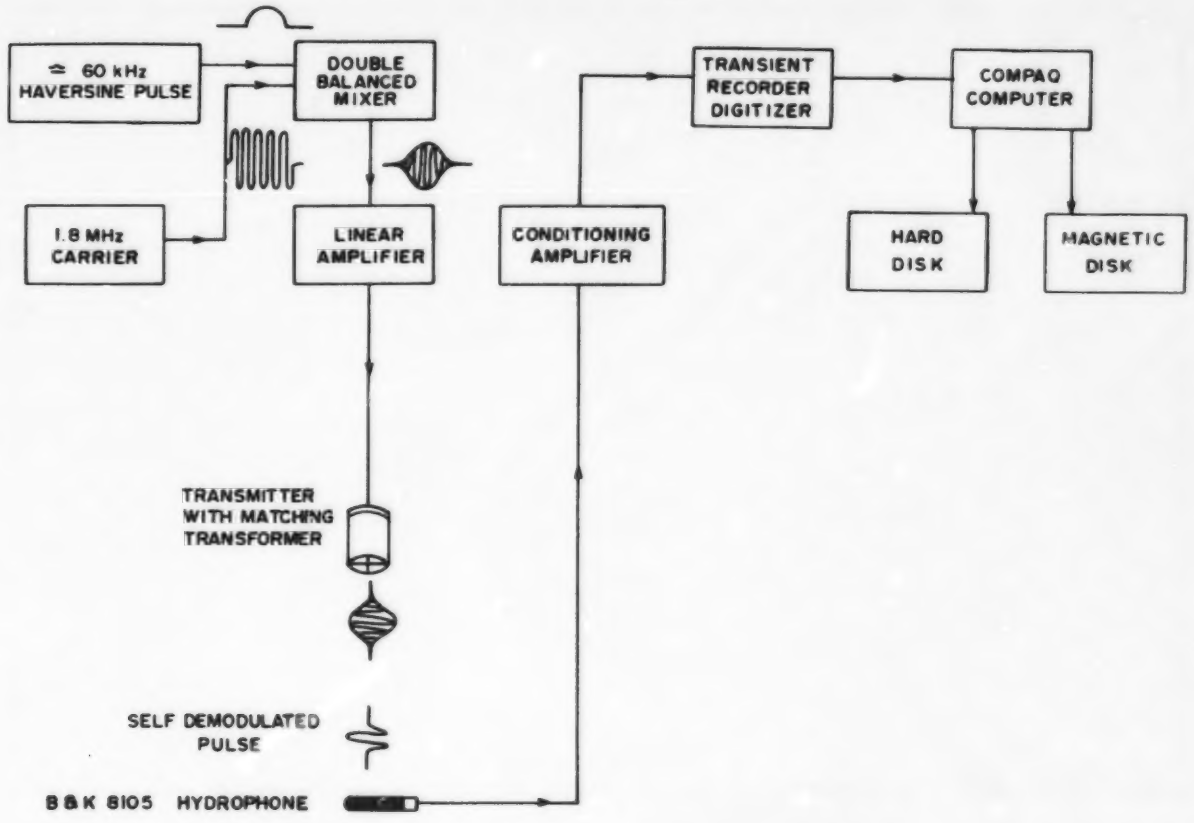

FIG. 2. Transmission and receiving schematic for parametric acoustic array.

of a broad band and narrow beam acoustic source, possessing central frequencies from 60 to 120 kHz derived using non-linear acoustics. The acoustic source together with a broad band hydrophone were mounted on an aluminum tripod. The face of the acoustic source was positioned at 70.3 cm above the tripod base. The hydrophone was placed 29.8 cm below and normal to the transducer face. A digital data acquisition system was used to acquire and process the data. The instrumentation setup used in this study is shown schematically in Figure 2. Acoustic data were collected at a site called Station 31 in Hamilton Harbour, Ontario (see Fig. 3).

TIME HISTORIES OF THE ACOUSTIC DATA

Figure 4 shows the acoustic records obtained with the parametric array. The data were collected using five different frequencies ranging from 60 kHz to 120 kHz in 20 kHz increments. The top portion of the figure shows 1,500 μs of data. The lower portion of Figure 4 shows an expanded section of the data from 600 to 1,500 μs. The following events are labelled in Figure 4 and a discussion pertaining to their significance is given on the basis of the acoustic data alone:

i) the event labelled "A" represents the direct arrival of the transmitted pulse at the hydrophone. The time of the first break was 210 μs. The transducer/hydrophone separation of 0.298 m permitted calculation of a sound velocity in water of 1,419 ms $^{-1}$.

ii) The event labelled B represents the first coherent reflected energy that was seen at all the traces. The 100 khz and 50 kHz records showed reflections prior to event B

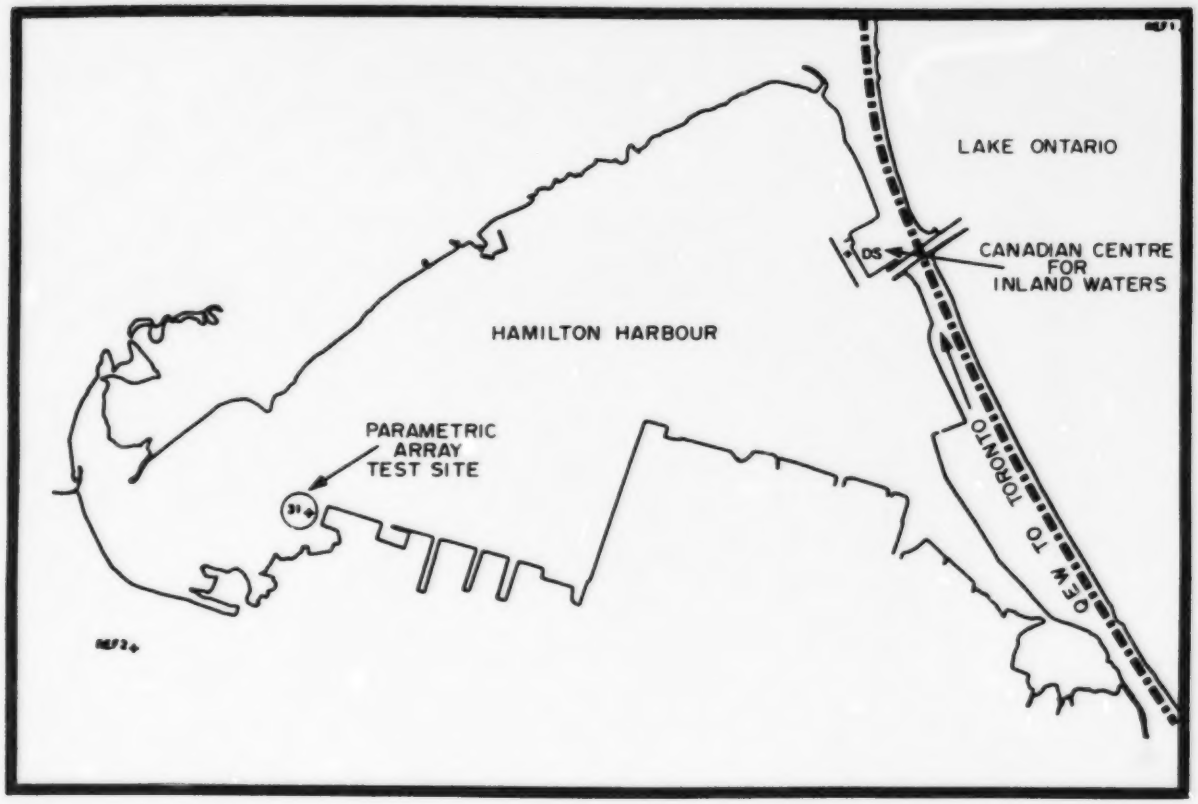

FIG. 3. Location of parametric array test site in Hamilton Harbour, Lake Ontario.

from particulates suspended in the water column. The low amplitude of the reflection at B suggested a boundary between water and a medium whose impedance was comparable to that of water. The calculated water velocity of 1,419 ms^{-1} and the reflection time of 710 μs placed this reflector at 65.3 cm. below the face of the transducer. This suggested that the tripod settled approximately 5 cm into the lakebed, given the transducer/tripod base distance of 70.3 cm.

iii) The event labelled "C" represents the lower boundary of the layer discussed in point (ii). This reflection was a replica of the direct arrival signal, suggesting a sharp interference between two media. The polarity of the reflection indicated a positive reflection coefficient, thus the material below "C" was of a higher impedance than the material above. The one way travel time between the events at "B" and "C" was 36 μs. This travel time, with a velocity similar to that of water, yielded a layer thickness of approximately 5 cm. The travel time to this horizon coincided with the travel time to the base of the tripod (assuming an average medium velocity of 1,419 ms^{-1}).

iv) The event labelled "D" represents the largest of the reflections present in the records. The large amplitude of the reflection denoted a high impedance contrast. The reflection had experienced some interference, suggesting either a gradational contact between the two media or the presence of point scatterers near the boundary. The one way travel time to "D" from the reflection at "C" was 24 μs. This travel time, together with the minimum

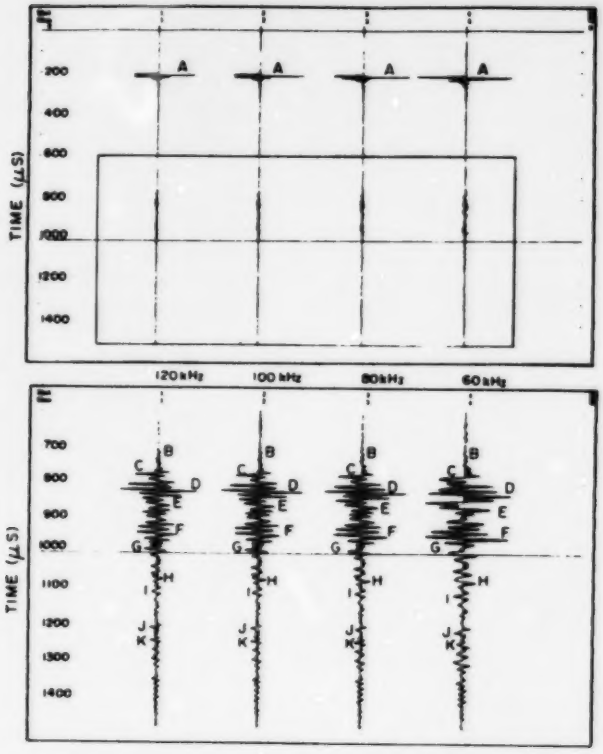

FIG. 4. Time histories of the acoustic pulse recorded at the test site using four different frequencies.

medium velocity for water, yielded a minimum layer of thickness of 3.5 cm.

v) The event labelled "E" represents a reflection at 888 μs. This placed the reflector 29 μs (one way travel time) below the reflector at "D." Using water velocity as a minimum, this layer was at least 4 cm thick.

vi) The event labelled "F" represents a reflection at 952 μs. The reverberant nature of the time histories near this event suggested either a gradational contact or the presence of point scatterers near the interface. The one way travel time of 32 μs from the reflection at "E" placed this boundary at approximately 4 cm below the reflector "E" (assuming velocity of sound in water). The interference made the determination of the polarity uncertain. The benefits of being able to operate at different frequencies are evident when comparing the reflection at F at different frequencies. The reflection at F on the 60 kHz trace was more pronounced than at the 120 kHz record.

vii) The events labelled "G," "H," "I," "J," and "K" represent reflectors respectively at 992 μs, 1,078 μs, 1,114 μs, 1,214 μs, and 1,252 μs. The reflections labelled "G" through "I" are real reflectors in the sub-surface. They may be due to point scatterers or gas bubbles, or might be representative of true stratigraphic boundaries. The event labelled "J" appears to be a real reflector since it is equivalent in amplitude to "K," where "K" is a multiple reflection of "D," and no other earlier reflection around "D" has a comparable amplitude. The reflection at "K" has a time (1,252 μs) equivalent to the travel time of a multiple reflection from the transducer face of the event labelled "D."

The events labelled in Figure 4 shift in time when viewed at different frequencies. This can be explained by the different temporal position of the peak in the direct wavelet at different frequencies as well as the dispersion in the water column. The ability to see the dispersive nature of the water column (see Fig. 5) and the sediments is a unique aspect of a parametric array source. Figure 5 shows the direct arrival of the acoustic pulse at the four different frequencies used during the survey. The lower portion of Figure 5 shows a comparison between the 100 kHz trace and a composite of the four different frequency traces that have been temporally adjusted such that the peak of each direct wavelength coincides. The benefits of summing the four different frequencies is most evident at reflector "F." The exact peak that represents "F" in the 100 kHz record is not as well pronounced as in the composite record.

INSTANTANEOUS AMPLITUDES

Figure 6 shows the instantaneous amplitudes of the time histories presented in Figure 4. The lower portion of Figure 6 illustrates an expanded portion of the records from 600 μs to 1,500 μs. Events are labelled as in Figure 4. An accurate time reference can be achieved using the Hilbert Transform of the real part of the signal to acquire the imaginary part. In this manner, the normal real valued time domain functions are made complex. From the transformation an envelope function is attained which can be displayed in a similar manner to functions in the frequency domain. The Hilbert Transform shifts each time component by 1/4

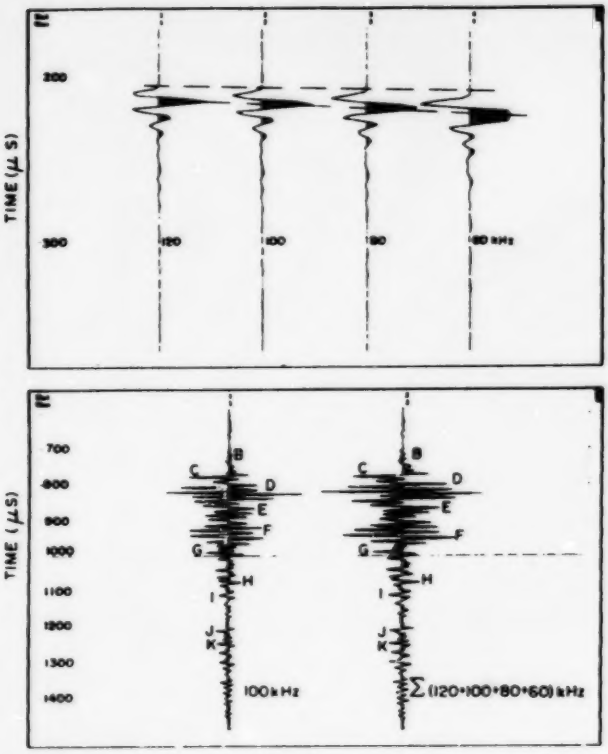

FIG. 5. Dispersion test of the water column (top). Frequency summation (bottom).

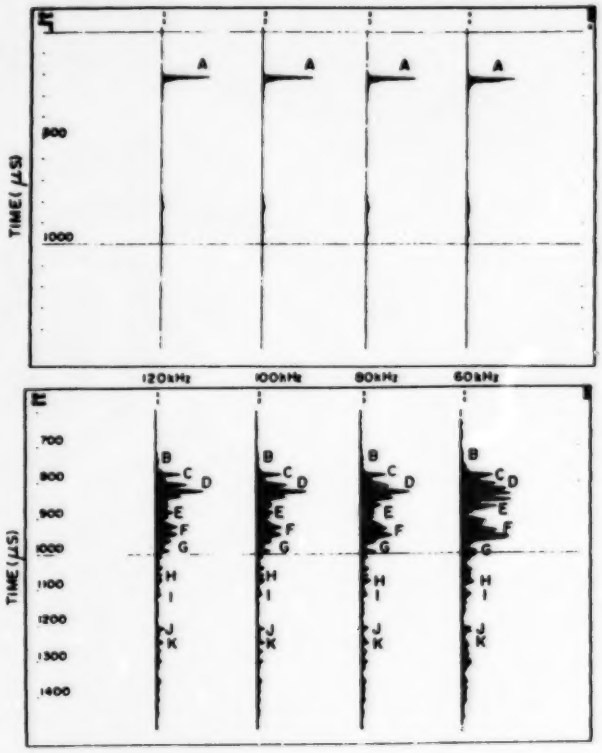

FIG. 6. Instantaneous amplitudes for time histories of the acoustic data recorded at test site using four different frequencies.

wavelength while it gives all frequency components a -90° phase shift, much like an integration of the signal. It is the resulting peak amplitude of the magnitude envelope which makes for an attractive time marker. The time "picks" in Figure 4 were made by applying the Hilbert Transform. The displayed instantaneous amplitudes represent a pseudo-energy envelope. The peaks in the reflected energy are easy to discern; for more details on the application of the Hilbert Transform to soundings refer to Guigné and Chin (1989).

Confidence in the Acoustic Records Acquired with a Parametric Source

The combination of a narrow beam acoustic pulse and a stationary open frame yielded free field and coherent conditions for the reflected signal. The first possible multiple reflection was an event reflected from the lakebed to the transducer and then to the hydrophone. Such a reflection would have to have travelled 1.604 m in the water column. Using the calculated water velocity of 1,419 m s^{-1} this reflection would have arrived at 1,130 μs. Hence, the events labelled A through I all occurred before such a time and must represent impedance contrasts in the sub-bottom. The absence of side lobe energy in the parametric array pulse also enhanced the recorded data and minimized the possibility of having spurious reflections in the profile.

Correlation Between Core and Acoustic Stratigraphy

Figure 7 shows the results of water content, grain size, and sand content analysis as measured from three cores taken at the location of the soundings (#31B, #31C, #31D – Rukavina 1990). An approximation of the stratigraphy was made based upon these analyses. From these core analyses the following can be deduced;

i) The high water content of the upper position of the cores together with the low sand

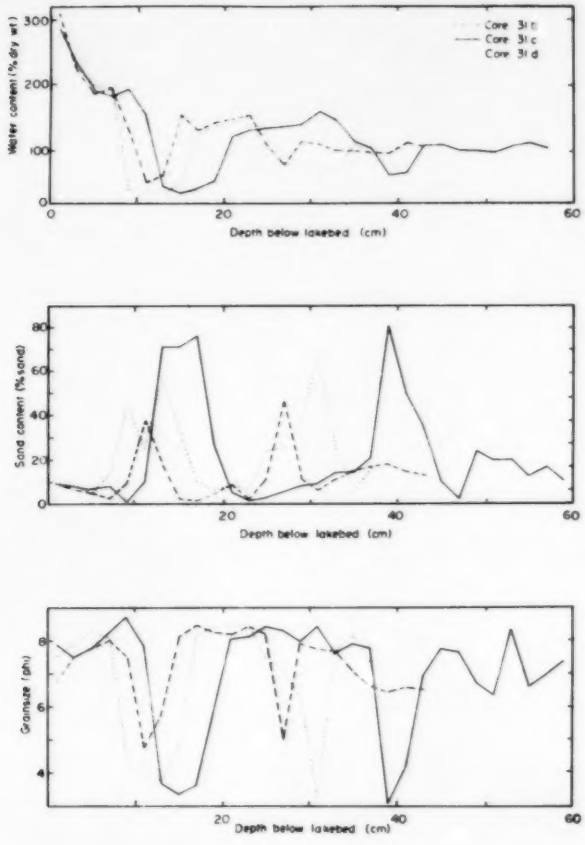

FIG. 7. Geotechnical analysis for water content (a), sand content (b), and grain size (c) of three cores collected at acoustic test site.

content constitute a boundary at the lakebed/water interface, which is characterized by a low acoustic reflectivity. This layer is indicative of the ooze present at the site.

ii) At the 4 cm depth, the water content remained constant for a short interval. The length of this interval varied from approximately 4 cm in cores 31B and 31D to approximately 7 cm in core 31C. Given the low sand content and moderately high water content this would appear to be a mud layer. Given the difference in water content, a moderate reflection could be expected from the top of this interface.

iii) All measured properties showed large discontinuities at depths ranging from 8 cm in cores 31B and 31D to approximately 10 cm in core 31C. The drop in water content together with the increases in sand content and grain size marked this as the top of a sand lens. Given the contrast in physical properties, a large reflection coefficient should exist at this interface.

iv) The bottom of the sand lens discussed in (iii) above ranged from approximately 14 cm in core 31B to approximately 20 cm in core 31C. This interface should also have exhibited a high impedance contrast. However the size of the reflection would be somewhat smaller than that at the top depending on how much energy was able to penetrate the upper boundary.

v) On the basis of the sand content and grain size data, a second sand lens could be seen. The location of the sand lens varied among the cores, although its thickness remained constant. The second sand lens could be seen at 26 cm depth from core 31B, 31cm depth in core 31D, and at 38 cm in core 31C. Normally, a sand lens provides for a high impedance contrast; however, the water content at this depth would lessen the strength of the boundary. In addition, reflections from this horizon could not be very large because of the inelastic attenuation experienced during the extended travel path.

Figure 8 shows the instantaneous amplitude of the summed frequency trace together with the water and sand content data from the core analyses. Joining lines represent correlations between the acoustic events and the core stratigraphy and reveal:

i) Reflection labelled "B" was the first arrival of coherent reflected energy at the hydrophone. The low reflection coefficient implied by the high water content was evident in the acoustic records. This reflection marked the top of the ooze layer.

ii) Reflection labelled "C" marked the base of the ooze layer. Given an acoustic velocity of 1,419 m s^{-1} in water and the 782 μs temporal position the reflector was 70.3 cm below the transducer face. Given the distance of 65.3 cm to the top of the layer this verified that the tripod settled 5 cm until it was supported by the layer beneath the ooze. The position of this reflection was consistent in all three cores.

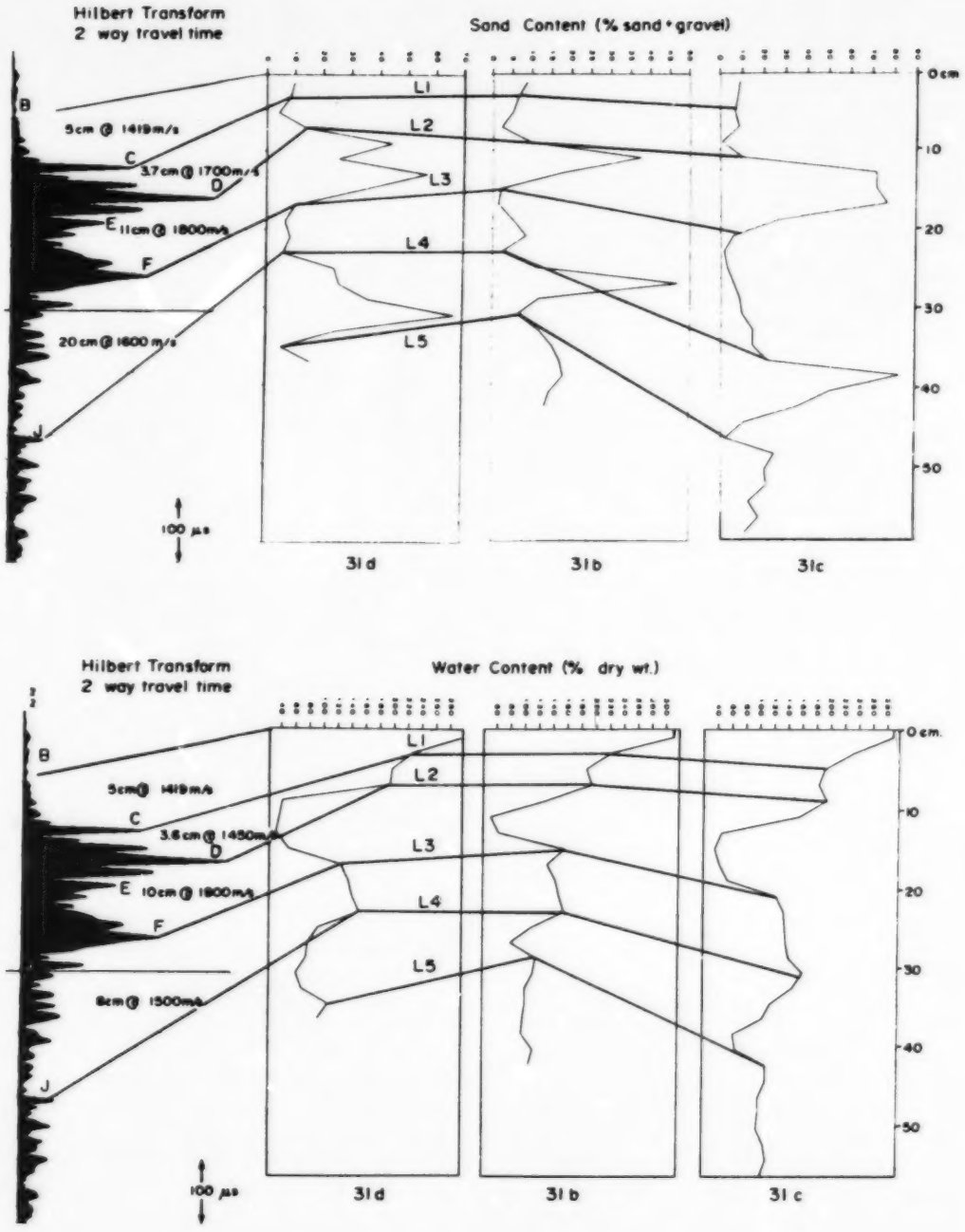

FIG. 8. Comparison of instantaneous amplitude of the acoustic data and the geotechnical analysis of the three cores collected at the test site.

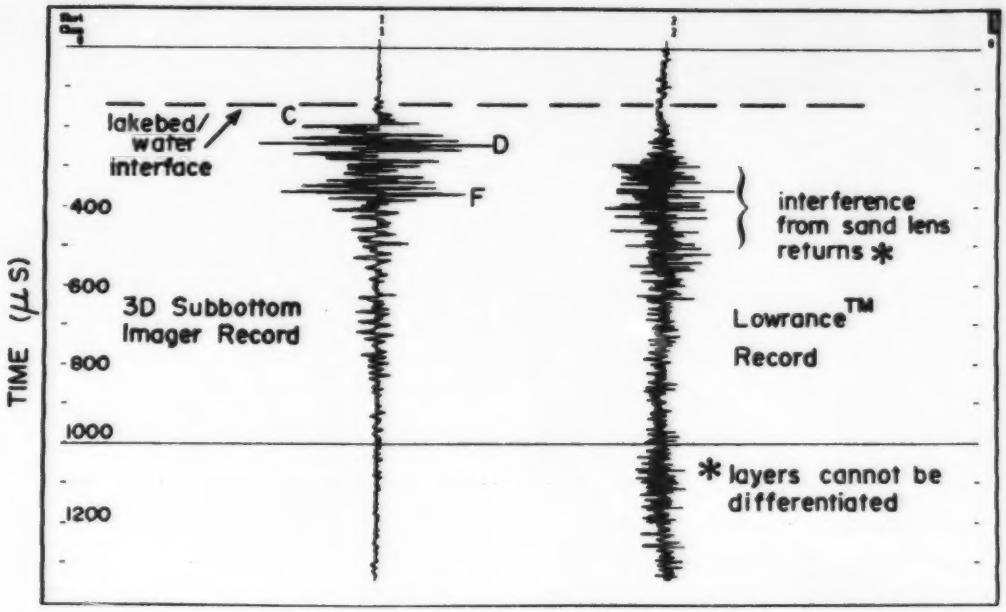

FIG. 9. Time histories of acoustic records from conventional echosounder and parametric sources.

iii) The reflector at "D" had the largest amplitude of all the reflections evident on the record. The apparent interference (in the form of multiple peaks) implied either a gradational boundary or the presence of scatterers near the interface. The strength of the reflection suggested a boundary with a high impedance contrast. Such conditions were present at the upper mud/sand interface in the cores. If the water velocity had been a minimum velocity possible for the material, and given a one way travel time of 24 μs, then the layer would have been 3.5 cm thick. A maximum velocity of 1,700 ms^{-1} would have given a layer thickness of 4.0 cm. This placed the bottom of the mud layer at approximately 8.5 cm depth. This coincided with the range of depths exhibited in the core data.

iv) Event "E" was a multiple reflection of the event "D" which travelled from "D," bounced once from "C," then returned to "D," and finally travelled upward toward the hydrophone. This was caused by the high reflectivity of reflectors "C" and "D."

v) The event labelled "F" was a strong reflector associated with the bottom of the sand lens. Again the interference pattern seen in Figure 4 indicated the presence of scatterers or a gradational boundary. A close examination of the record on Figure 4 showed a significant drop in the amplitude of the energy envelope. This decrease in energy was related to the high reflectivity of the sand lens coupled with the large inelastic attenuation associated with sands. The 61 μs one way travel time together with a minimum medium velocity of 1,419 m s^{-1} yielded a minimum layer thickness of 8.6 cm, placing the bottom of the sand lens at a depth of 17 cm. Assuming a maximum velocity of 1,800 m s^{-1}, the sand lens would have been 11 cm thick, thus placing the bottom of the sand lens at 19 cm. Both of these estimates fell within the core data statistics.

vi) The event labelled "J" appeared to be the top of the lower sand lens. A strong reflectivity was expected at this interface. Given the interbedding of sand and mud, an average velocity to the lower sand lens of 1,600 ms^{-1} would have been reasonable. The two way travel time from the lakebed interface

and the reflection from the top of the sand lens would have been 500 μs. This two way travel time was consistent with the reflector at "J."

Figure 9 shows the summed frequency trace of the parametric array and a trace recorded by a representative echosounder (Lowrance™) for the same location. The dashed line represents the approximate site of the bottom based upon tripod geometries and calculated water velocities. The records from the Lowrance™ had an interference pattern caused by its overlapping returns from the top and bottom of the sand lens. The record also demonstrated a high noise content. The short pulse length of the parametric array, as well as the absence of side-lobe energy, illustrated the precision in imaging fine stratigraphic structures using principles of non-linear acoustics.

CONCLUSIONS

The acoustic data described in this paper show the merits of using a parametric array for sub-bottom profiling of sediments when high resolution is required. The temporal resolution obtained with the parametric source was not achievable with a conventional source. This ability to detect and resolve thin layers in modern contaminated sediments like those of Hamilton Harbour has important applications for the research and management of polluted sediments. In its current form the equipment could be used to monitor sedimentation processes and rates remotely as an aid to understanding the transport and accumulation of polluted sediments. With further development it might also be useful in a survey mode for fast, high-resolution mapping of the thickness and distribution of polluted sediments.

ACKNOWLEDGMENTS

The experiment discussed in this paper was undertaken under the auspices of a program with the National Water Research Institute (NWRI) of Burlington, Ontario (Guigné *et al.* 1990). Funding for this project was jointly provided by Environment Canada under Dr. Norman Rukavina's leadership and by Dr. Guigné's NSERC (Natural Sciences and Engineering Research Council of Canada) Operating Grant. The authors would like to extend thanks to Mr. Brian Trapp of NWRI as well as Mr. Voon H. Chin of C-CORE. We would also like to thank the crew of the research vessel *MV Shark* for their support during data collection.

REFERENCES

Berktay, H. O. 1965. Possible exploitation of non-linear acoustics in underwater transmitting applications. *J. Sound. Vib.* 2(4):435–461.

_____, Smith, B. V., Braithwaite, H. B., and Whitehouse, M. 1979. Sub-bottom Profilers with Parametric Sources. Underwater Applications in Underwater Acoustics. Session 1.2, 1–10, Institute of Acoustics, University of Bath, England.

Ceen, R. V., and Pace, N. G. 1981. Time Domain Study of the Terminated Parametric Array. Advancements in Underwater Acoustics, Session 6, 1–10, Institute of Acoustics, University of Bath, England.

Fass, R. W. 1969. Analysis of the relationship between acoustic reflectivity and sediment porosity. *Geophysics* 34:546–553.

Guigné, J. Y. 1986. The concept, design and experimental evaluation of an acoustic sub-sealed interrogator, pp. 37–144. Ph.D. thesis, University of Bath, England.

_____, and Chin, V. H. 1989. Acoustic imaging of an inhomogenous sediment matrix. *Marine Geophysical Researches* 11:301–317.

_____, Pace, N. G., and Chin, V. H. 1989. Dynamic extraction of attenuation from sub-bottom acoustic data. *J. Geophys. Res.* 94:5745–5755.

_____, Hunt, P. H., and Solomon, S. 1990. *Sub-bottom imaging with a parametric array source in Hamilton Harbour*, pp. 1–43. Contract report for the Department of the Environment; National Water Research Institute.

Hamilton, E. L. 1971. Elastic properties of marine sediments. *J. Geophys. Res.* 76:579–604.

_____. 1972. Compressional wave attenuation in marine sediments. *Geophysics* 37:620–646.

_____. 1974. *Prediction of Deep-sea Sediments Properties: State of the Art in Deep Sea Sediments, Physical and Mechanical Properties*, Ed. A. L. Inderbizen, Plenum I, Vol. 2, pp: 1–43.

_____, and Bachman, R. T. 1982. Sound velocity and related properties of marine sediments. *J. Accoust. Soc. Am.* 72:1891–1903.

Orr, M. H., and Rhoads, D. C. 1982. Acoustic imaging of structures in the upper 10 cm of sediments using a megahertz backscattering system: preliminary results. *Marine Geology* 46:117–129.

Pace, N. G., and Ceen, R. V. 1982. Seabed classification using backscattering of normally incident broadband acoustic energy. *Hydrographic Journal* 26:9–16.

_____, and Ceen, R. V. 1983. Time domain study of the terminated parametric array, *J. Acoust. Soc. Am.* 73:1972–1978.

Rukavina, N. A. 1990. *Geotechnical properties of Hamilton Harbour cores at acoustic test sites, October 1989*. National Water Research Institute, Lakes Research Branch Technical Note LBR-90-TN-08.

Smithy, D. T., and Li, W. N. 1966. Echo soundings and sea floor sediments. *Marine Geology* 4:353–364.

Telford, W. M., Geldart, L. P., Sherriff, R. E., and Keys, D. A. 1976. Seismic Theory. In *Applied Geophysics*, pp. 222–257. Cambridge; Press Syndicate of the University of Cambridge.

Westervelt, P. J. 1963. Parametric acoustic array. *J. Acoust. Soc. Am.* 35:535–537.